Uranium and radium diffusion in organic-rich sediments (sapropels)

A. Gourgiotis, J.-L. Reyss, N. Frank, Abel Guihou, C. Anagnostou

Geochemistry Geophysics Geosystems G3

Article
Volume 12, Number 9
21 September 2011
Q09012, doi:10.1029/2011GC003646
ISSN: 1525-2027

Published by AGU and the Geochemical Society

Uranium and radium diffusion in organic-rich sediments (sapropels)

A. Gourgiotis, J.-L. Reyss, and N. Frank
Laboratoire des Sciences du Climat et de l'Environnement, Vallée Bâtiment 12, avenue de la Terrasse, F-91198 Gif-sur-Yvette CEDEX, France (alkis.gourgiotis@lsce.ipsl.fr)

A. Guihou
Lamont Doherty Earth Observatory, Columbia University, 61 Route 9W, Palisades, New York 10964-8000, USA

C. Anagnostou
Hellenic Centre for Marine Research, Institute of Oceanography, 46.7 km Athens-Sounio Avenue, GR-19013 Anavyssos, Attiki, Greece

[1] Among the late Quaternary Mediterranean sapropels, the S5 (125 ka) is one of the best preserved due to its high organic carbon content that has limited postdepositional oxidation. The high uranium content in this sapropel, >40 dpm g^{-1}, makes this layer interesting for studying uranium series disequilibrium in organic-rich sediments. For this reason, the present work provides isotopic measurements of the U decay series in a S5 sapropel by applying more precise mass spectrometric methods, TIMS/MC-ICPMS, and gamma spectrometry. Assuming that U in the sapropel mostly originated from seawater the ($^{234}U/^{238}U$), ($^{230}Th/^{238}U$), ($^{226}Ra/^{230}Th$) and ($^{231}Pa/^{235}U$) activity ratios show systematic deviations from the theoretical values for a closed-system evolution of the U series over the 125 ka since sapropel formation. The radiogenic $^{234}U_{rad}$ and ^{226}Ra show clear evidence of migration in the sapropel with modeled diffusion coefficients of $(7.1 \pm 1.1) \times 10^{-12}$ cm^2 s^{-1} and $(1.6 \pm 0.2) \times 10^{-10}$ cm^2 s^{-1}, respectively. The diffusion of $^{234}U_{rad}$ cannot explain the high ($^{230}Th/^{238}U$) and ($^{231}Pa/^{235}U$) activity ratios observed in the sapropel. Two possible mechanisms or a combination of both are proposed for explaining the irregular ($^{230}Th/^{238}U$) and ($^{231}Pa/^{235}U$) activity profiles in sapropel S5. The first one is an enhanced export flux of $^{230}Th_{xs}$ and $^{231}Pa_{xs}$ excesses exceeding the production rate in seawater, during the time of sapropel formation, and the second one is diffusion of authigenic U_{auth} in the sapropel. However, the ambiguous determination of $^{230}Th_{xs}$ and $^{231}Pa_{xs}$ in the sapropel and the poorly understood processes that might lead to U_{auth} migration in anoxic sediments still limit a final explanation for the deviation of ($^{230}Th/^{238}U$) and ($^{231}Pa/^{235}U$) activity ratios from their expected theoretical values.

Components: 9700 words, 6 figures, 2 tables.

Keywords: Radium; diffusion; protactinium; sarpopels; sediments; uranium.

Index Terms: 1040 Geochemistry: Radiogenic isotope geochemistry; 1051 Geochemistry: Sedimentary geochemistry; 1120 Geochronology: Isotopic disequilibrium dating.

Received 1 April 2011; **Revised** 27 July 2011; **Accepted** 28 July 2011; **Published** 21 September 2011.

Gourgiotis, A., J.-L. Reyss, N. Frank, A. Guihou, and C. Anagnostou (2011), Uranium and radium diffusion in organic-rich sediments (sapropels), *Geochem. Geophys. Geosyst.*, *12*, Q09012, doi:10.1029/2011GC003646.

1. Introduction

[2] Sediment cores from the eastern Mediterranean Sea contain numerous dark colored layers rich in organic carbon and commonly laminated. These organic-rich layers are called sapropels (from the Greek sapros → rotten and pelos → soil) provided their thickness exceeds 1 cm and the total organic carbon (C_{org}) content exceeds 2% [*Kidd et al.*, 1978]. Among the late Quaternary Mediterranean sapropels (S1 to S11), the S5 (125 ka) is one of the best preserved due to its high organic carbon content [*Löwemark et al.*, 2006]. Two different models have been proposed for sapropel formation. The first one is the stagnation model that assumes that reduced or nonexistent deep-water ventilation, due to stratification of the water column, leads to anoxic conditions at seafloor and consequently to preservation of organic material [*Aksu et al.*, 1995; *Cita et al.*, 1977; *Thunell and Williams*, 1989]. The second one is the productivity model, which proposes elevated primary production due to the increased nutrient availability in the surface water [*Castradori*, 1993; *De Lange and ten Haven*, 1983]. A combination of these two models, reduced deep-water ventilation and increased productivity in the surface water, has been proposed by more recent studies [*Emeis et al.*, 2000a, 2000b; *Rohling*, 1994; *Warning and Brumsack*, 2000].

[3] The chronology of the sapropel layers has previously been determined by oxygen isotope stratigraphy, biostratigraphy, tephrochronology and radiocarbon ^{14}C dating for the youngest ones [*Hilgen*, 1991; *Jorissen et al.*, 1993; *Lourens et al.*, 1996; *Paterne et al.*, 1986; *Thomson*, 1982]. Pioneering work based on alpha spectrometry, by *Mangini and Dominik* [1979] and later by *Severmann and Thomson* [1998], tried to use U series daughters (U/Th) in order to provide more accurate and precise sapropel ages. However, precise U series chronologies were not achieved due to postdepositional diagenesis leading to open-system evolution of the U-series nuclides in sapropels. *Severmann and Thomson* [1998] proposed the $^{231}Pa/^{235}U$ dating technique as a possible alternative for dating sapropels but the much lower detection limits required for ^{235}U and ^{231}Pa are not easily achievable by traditional alpha spectrometry.

[4] This work provides isotopic analysis of the U series nuclides (^{238}U, ^{234}U, ^{235}U, ^{230}Th, ^{232}Th, ^{231}Pa) for one Mediterranean S5 sapropel by using mass spectrometric methods, TIMS and MC-ICPMS. In addition, ^{226}Ra activities were acquired using low level gamma spectrometry. The Mn and organic contents of the sapropel and overlying sediments were also measured.

[5] In the following, the activity ratio distributions of ($^{234}U/^{238}U$), ($^{230}Th/^{238}U$), ($^{226}Ra/^{230}Th$) and ($^{231}Pa/^{235}U$) are discussed in comparison with the expected theoretical closed system of the U series nuclides under the presumption of a seawater uranium origin. Our objective is to shed new light on the diffusion of radionuclides in organic-rich sediments and to refine the diffusion coefficients needed to potentially date such archives using U series open-system models in the future.

2. Material and Methods

[6] Here, we have investigated in great detail the so-called S5 sapropel (125 ka) from a gravity core (ADE3–24) collected in the Eastern Mediterranean sea (33°66′N, 20°86′E) at a depth of 2630 m. The core (2.45 m long) sealed in a PVC liner was stored in a constant temperature room (~10°C) for one year. One hour after the core opening in the laboratory, the sapropel layer was sampled every cm. All samples were dried at 50°C and ground in an agate mortar and sealed in plastic tubes for further geochemical analysis.

[7] In this core, the S5 sapropel is 11.5 cm thick, faintly laminated layer, and it is located between the core depths 214.0 cm and 225.5 cm.

[8] For U-Th analysis, the total sample dissolution method was used and all samples were spiked with a mixed ^{233}U-^{236}U-^{229}Th spike. U and Th were separated and purified by ion-exchange chemistry [*Lawrence et al.*, 1987] and were deposited on rhenium filaments. The samples were analyzed using a thermal ionization mass spectrometer (Finnigan MAT262) at LSCE–Gif-sur-Yvette. Mass fractionation of $^{234}U/^{235}U$ isotopic ratio and ^{235}U concentrations were estimated using the known $^{233}U/^{236}U$ ratio and ^{236}U concentration in the spike, respectively.

[9] For thorium isotope ratio measurement the $^{232}Th/^{229}Th$ and $^{229}Th/^{230}Th$ ratios were measured separately (in a two different runs) due to the high ^{232}Th abundance, and no corrections for isotope ratio fractionation were applied. For the $^{230}Th/^{238}U$ isotope ratio an external correction (linear law) was done by using a sample-standard bracketing procedure every two samples. The bracketing procedure was performed by using the HU-1 reference material and the values reported by *Cheng et al.* [2000]. The

reproducibility of ($^{234}U/^{238}U$) activity ratios and U concentrations are better than 4‰ and that of ($^{230}Th/^{238}U$) activity ratios are better than 8‰.

[10] Full procedural blanks had an average value of 3.8 ng for ^{238}U, 30 fg for ^{230}Th and 0.3 ng for ^{232}Th and are negligible with respect to the amounts of ^{238}U, ^{234}U, ^{230}Th and ^{232}Th in the analyzed sample aliquot.

[11] For ^{226}Ra nuclide determination, powdered samples weighing between 1.8 g and 2 g were sealed in plastic cylindrical tubes and were analyzed at the underground laboratory of Modane (Laboratoire Souterrain de Modane, French Alps) by using low level gamma spectrometry. High-efficiency, low-background, well-type germanium detectors (430 cm^3 and 950 cm^3 active volume) were used [*Reyss et al.*, 1995]. These detectors are shielded from cosmic radiation by 1700 m of rocks, which results in very low background less than 0.6 cpm between 30 and 2700 keV. Because ^{226}Ra activity is determined from the ^{214}Pb (295 and 352 keV) and ^{214}Bi (609 keV) peaks, gamma analyses were performed about one month after the samples were sealed in order to assure ensure radioactive equilibrium between the isotopes.

[12] ^{231}Pa measurements were carried out using about 50 mg of sediment for each sample. The samples were spiked with ^{233}Pa and ^{236}U prior to total digestion. The Pa and U fractions were separated and purified using anion exchange chromatography AG1x8 BioRad® [*Guihou et al.*, 2010]. The Pa and U fractions were analyzed using a MC-ICPMS (Nu 500 HR at Laboratoire de Géologie de Lyon, Ecole Normale Supérieure de Lyon, France). Ratios were corrected for instrumental background noise, blank contributions and tailing of ^{232}Th on mass 231 and 233. The overall correction was below 5% for Pa and 5‰ for U. The instrumental mass bias was monitored by standard bracketing with the IRMM 184 uranium isotopic standard.

[13] Mn contents were determined using X-ray micro fluorescence with a iMOXS X-ray source combined to a JEOL 840 Scanning Electron Microscope (SEM). Multielement spectra were obtained with an Energy Dispersive Spectrometer (EDS) equipped with a high purity Ge detector from PGT. X-ray micro fluorescence analyses were performed on a few milligrams of compacted sediment powders and USGS rocks were used as standards. No specific sample preparation was required.

[14] For organic carbon analyses two different measurements were done on each sediment sample: total carbon on bulk sediment, and organic carbon after sediment leaching with 0.6N HCl for 3–4 days until no further gas bubbling is recognized. About 15–20 mg of sediment was weighed using tin cups for measurement (with a precision of 1 μg). The sample was combusted in a Fisons Instrument NA 1500 Element Analyzer and carbon content determined by the Eager software. An acetanilide standard (71.07%wt of carbon) was inserted every 10 samples. Assuming that mineral carbon exists only in the form $CaCO_3$, the organic carbon content in bulk sediment was deduced. Results are reported in weight % of organic carbon/bulk sediment.

3. Results and Discussion

3.1. Uranium Series Radionuclide Profiles in the S5 Sapropel

[15] High organic carbon (C_{org}) contents and high uranium (^{234}U, ^{238}U) activities are observed in the sapropel unit compared with the surroundings sediments (Figures 1a and 1b; see also Table 1). The high uranium activities are the result of anoxic conditions prevailing during sapropel formation. Dissolved seawater U(VI+) is reduced to U(IV+) under anoxic conditions and is removed from solution into marine sediments [*Anderson et al.*, 1989a; *Barnes and Cochran*, 1990; *Barnes and Cochran*, 1991; *Cochran et al.*, 1986; *Klinkhammer and Palmer*, 1991; *McManus et al.*, 2005]. However, particulate nonlithogenic uranium has been observed in the Santa Barbara Basin sediment showing evidence for an association of U with organic matter in seawater [*Zheng et al.*, 2002]. We consider that during uranium removal from seawater, either by precipitation in the sediments and/or in form of particulate nonlithogenic uranium, no significant isotopic fractionation between ^{234}U and ^{238}U is observed. Therefore, the seawater-derived uranium in the sediments acquires the isotopic fingerprint of seawater with a ($^{234}U/^{238}U$) activity ratio equal to 1.147 [*Andersen et al.*, 2010; *Chen et al.*, 1986]. This uranium is called authigenic (U_{auth}) and is the most important uranium fraction in Mediterranean sapropels [*Mangini and Dominik*, 1979; *Severmann and Thomson*, 1998; *Thomson*, 1982]. U_{auth} dominates largely over the detrital uranium (U_{det}) originating from mineral lattices of the terrigenious sediment fraction. However, this view for a marine origin of uranium in sapropels has been challenged by *Bernat et al.* [1989] who suggested that the uranium is derived almost entirely from terrigenous material [*Bernat et al.*, 1989].

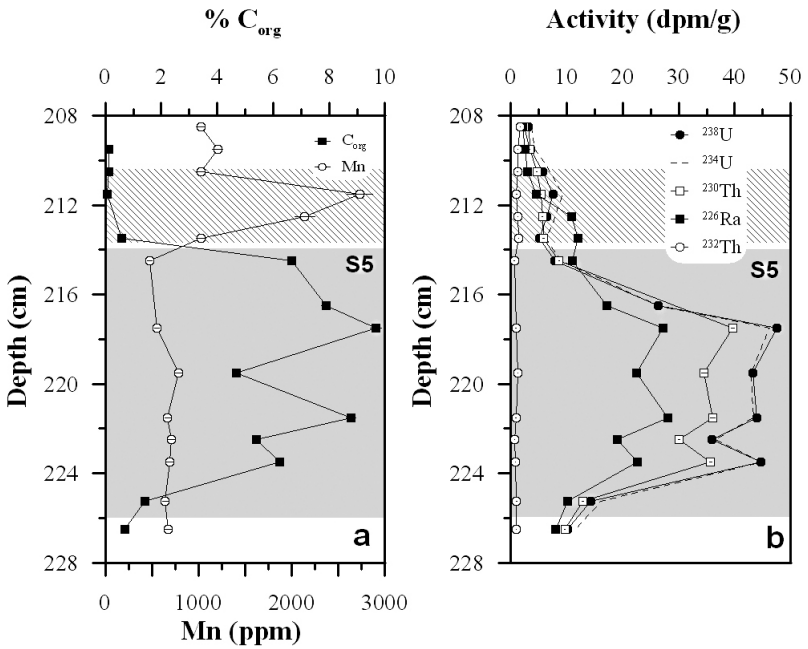

Figure 1. Vertical distribution of (a) Mn and C_{org} and (b) ^{238}U decay products and ^{232}Th in the studied core. The Mn-rich zone and the sapropel unit are marked by the striped and the shaded areas, respectively. Error bars are included in the symbols and are expressed at a 95% confidence level.

[16] In contrast to the uranium in the sapropels, ^{232}Th is primordial and exclusively derived from detrital material of erosional debris. ^{232}Th activity in the sapropel is consistently lower than 1.3 dpm g^{-1} with little variation with depth. (Figure 1b).

[17] Sedimentary ^{230}Th consists of three distinct sources: (1) detrital $^{230}Th_{det}$ from terrigenous minerals, (2) nonsupported excess of $^{230}Th_{xs}$ produced in seawater from the decay of dissolved ^{234}U, and (3) authigenic $^{230}Th_{auth}$ produced within the sediments from radioactive decay of $^{234}U_{auth}$. Because $^{230}Th_{xs}$ is rapidly scavenged from the water column by adsorption on the surfaces of sinking particles, the flux of $^{230}Th_{xs}$ to the seafloor is considered to be close to its rate of production by ^{234}U decay in the overlying water column [*Henderson et al.*, 1999a; *Yu et al.*, 2001]. Once stored in the sediment, $^{230}Th_{xs}$ decays according to its half-life of 75.7 ka. Due to high $^{234}U_{auth}$ activities in sapropel and because of the age of S5 (125 ka), sufficient time has elapsed leading to a distinct ingrowth of the ^{230}Th activity toward radioactive equilibrium with ^{234}U. This leads to ^{234}U and ^{230}Th profiles, which are rather similar (Figure 1b).

[18] Like ^{230}Th, three different sources for sedimentary ^{226}Ra have also to be distinguished: (1) detrital $^{226}Ra_{det}$ locked in the mineral lattices of erosional debris, (2) $^{226}Ra_{xs}$ derived from the seawater by in situ formed settling barite minerals [*Bishop*, 1988; *Stroobants et al.*, 1991], and (3) authigenic $^{226}Ra_{auth}$ produced in sediment by radioactive decay of ^{230}Th ($^{230}Th_{auth}$ and/or $^{230}Th_{xs}$). $^{226}Ra_{xs}$ decays with a half-life of 1.6 ka and thus in S5 sapropel has totally decayed, such that ^{226}Ra should be in secular equilibrium with ^{230}Th. ^{226}Ra activity profile in the sapropel is similar to that of ^{230}Th due to the ingrowth of $^{226}Ra_{auth}$ activity toward radioactive equilibrium with ^{230}Th (Figure 1b).

3.2. Evidence for Postdepositional Diffusion of Uranium Decay Products

3.2.1. Authigenic Versus Detrital Sources in the S5 Sapropel

[19] Activity ratios for the detrital component in the sapropel are estimated from the measured ^{232}Th activity and an inferred ($^{238}U_{det}/^{232}Th$) activity ratio for the detrital material, assuming that all decay products of ^{238}U are in secular equilibrium, hence ($^{238}U_{det}$) = ($^{234}U_{det}$) = ($^{230}Th_{det}$) = ($^{226}Ra_{det}$). The detrital ($^{238}U_{det}/^{232}Th$) activity ratio for the eastern Mediterranean Sea used in this work is equal to 0.76 ± 0.1 [*Thomson*, 1982]. This value is in a good agreement with previous in-house measurements of Mediterranean sediment cores (0.69–0.83, J.-L. Reyss, unpublished data, 2004). Broadly similar mean ($^{238}U_{det}/^{232}Th$) activity ratios have also been suggested for Atlantic (0.6 ± 0.1), Pacific (0.7 ± 0.1)

Table 1. Summary of C_{org}, Mn, and U Series Isotopic Data for the S5 Sapropel[a]

Depth (cm)	Corg (%)	Mn (ppm)	^{232}Th (dpm/g)	^{238}U (dpm/g)	^{230}Th (dpm/g)	^{226}Ra (dpm/g)	^{231}Pa (dpm/g)	^{234}U/^{238}U Activity Ratio	^{230}Th/^{238}U Activity Ratio	^{230}Th/^{234}U Activity Ratio	^{226}Ra/^{230}Th Activity Ratio	^{231}Pa/^{235}U Activity Ratio
208.5		1023 ± 48	1.63 ± 0.02	3.117 ± 0.008	2.35 ± 0.27	2.17 ± 0.05		1.182 ± 0.013	0.755 ± 0.086	0.639 ± 0.073	0.92 ± 0.11	
209.5	0.129 ± 0.003	1205 ± 56	1.26 ± 0.02	3.617 ± 0.004	3.36 ± 0.04	2.51 ± 0.12		1.191 ± 0.006	0.930 ± 0.012	0.781 ± 0.011	0.75 ± 0.04	
210.5	0.130 ± 0.003	1023 ± 48	1.19 ± 0.01	5.778 ± 0.007	4.64 ± 0.05	3.01 ± 0.09		1.218 ± 0.004	0.803 ± 0.008	0.660 ± 0.007	0.65 ± 0.02	
211.5	0.064 ± 0.001	2730 ± 136	1.05 ± 0.01	7.537 ± 0.010	5.36 ± 0.11	4.50 ± 0.12		1.221 ± 0.004	0.711 ± 0.014	0.582 ± 0.012	0.84 ± 0.03	
212.5		2138 ± 106	1.20 ± 0.01	6.482 ± 0.013	5.64 ± 0.04	10.91 ± 0.23		1.231 ± 0.006	0.869 ± 0.007	0.706 ± 0.006	1.94 ± 0.04	
213.5	0.596 ± 0.012	1026 ± 51	1.44 ± 0.04	5.165 ± 0.010	5.85 ± 0.14	11.99 ± 0.26		1.213 ± 0.006	1.133 ± 0.028	0.934 ± 0.024	2.05 ± 0.07	
214.5	**6.652 ± 0.133**	**478 ± 25**	**0.63 ± 0.03**	**7.821 ± 0.011**	**8.61 ± 0.08**	**11.03 ± 0.24**		**1.147 ± 0.009**	**1.101 ± 0.010**	**0.960 ± 0.011**	**1.28 ± 0.03**	
216.5	**7.890 ± 0.158**		**0.91 ± 0.01**	**26.270 ± 0.165**		**17.20 ± 0.30**		**0.999 ± 0.009**				
217.5	**9.672 ± 0.193**	**555 ± 29**	**1.29 ± 0.03**	**47.570 ± 0.081**	**39.67 ± 0.25**	**27.20 ± 0.30**	**2.09 ± 0.06**	**0.971 ± 0.004**	**0.834 ± 0.005**	**0.859 ± 0.006**	**0.69 ± 0.01**	**0.953 ± 0.027**
219.5	**4.670 ± 0.093**	**784 ± 39**	**0.90 ± 0.02**	**43.248 ± 0.030**	**34.58 ± 0.46**	**22.51 ± 0.32**	**2.27 ± 0.05**	**0.992 ± 0.006**	**0.800 ± 0.011**	**0.807 ± 0.012**	**0.65 ± 0.01**	**1.137 ± 0.024**
221.5	**8.774 ± 0.175**	**670 ± 33**	**0.73 ± 0.01**	**43.944 ± 0.011**	**36.10 ± 0.37**	**28.12 ± 0.48**	**2.51 ± 0.05**	**0.987 ± 0.005**	**0.821 ± 0.008**	**0.832 ± 0.009**	**0.78 ± 0.02**	**1.239 ± 0.026**
222.5	**5.410 ± 0.108**	**708 ± 36**	**0.83 ± 0.01**	**35.941 ± 0.072**	**30.04 ± 0.19**	**19.00 ± 0.30**		**1.015 ± 0.004**	**0.836 ± 0.005**	**0.824 ± 0.006**	**0.63 ± 0.01**	
223.5	**6.224 ± 0.124**	**691 ± 5**	**1.04 ± 0.02**	**44.657 ± 0.014**	**35.68 ± 0.18**	**22.60 ± 0.30**	**2.02 ± 0.05**	**1.002 ± 0.004**	**0.799 ± 0.004**	**0.797 ± 0.005**	**0.63 ± 0.01**	**0.979 ± 0.025**
225.25	**1.430 ± 0.029**	**641 ± 32**	**0.96 ± 0.01**	**14.331 ± 0.023**	**12.83 ± 0.15**	**10.20 ± 0.30**		**1.123 ± 0.007**	**0.895 ± 0.010**	**0.797 ± 0.010**	**0.80 ± 0.03**	
226.5	0.699 ± 0.014	671 ± 34	3.95 ± 0.04	10.172 ± 0.033	9.69 ± 0.09	7.92 ± 0.23		1.135 ± 0.006	0.953 ± 0.009	0.839 ± 0.009	0.82 ± 0.02	

[a]Samples that comprise the sapropel unit are shown in bold. Weighting errors are taken into account for concentrations and activities final error calculation. Errors are expressed at a 95% confidence level.

and Southern Ocean (0.4 ± 0.1) [*Henderson and Anderson*, 2003]. The calculated average contribution of the detrital fraction to the total activities of ^{234}U, ^{238}U, ^{230}Th and ^{226}Ra of the sapropel is < 4%. Furthermore, if the assumption for secular equilibrium between the decay products of $^{238}U_{det}$ is not respected due to the alpha recoil effect [*Fleischer*, 1988], the $(^{234}U/^{238}U)_{det}$, $(^{230}Th/^{238}U)_{det}$, $(^{226}Ra/^{238}U)_{det}$ activity ratios should be <1. In this case, the detrital faction contribution to the total activities of the isotopes is even smaller. The relative difference between uncorrected and detrital-free activity ratios is found to be <0.8% for $(^{234}U/^{238}U)$ and $(^{230}Th/^{238}U)$ and <1.7% for $(^{226}Ra/^{230}Th)$. This difference is within the analytical errors of the activity ratios and thus the detrital contribution in the sapropel can be neglected.

3.2.2. Radiogenic $^{234}U_{rad}$ Diffusion

[20] The primary control on the $(^{234}U/^{238}U)$ activity ratio in the sapropel at the time of its formation is the relative contribution of authigenic and detrital U. As mentioned above, the detrital contribution does not significantly change this ratio in the S5 sapropel. Therefore, the $(^{234}U/^{238}U)$ activity ratio in the S5 sapropel is mostly controlled by authigenic uranium that has acquired the isotopic fingerprint of the seawater that prevailed during sapropel formation. Considering that the seawater $(^{234}U/^{238}U)$ activity ratio was presumably identical to the one of modern seawater (1.147) for the period of time that covers the age of S5 sapropel [*Henderson*, 2002], the theoretical activity ratio expected from radioactive decay of ^{234}U and for a closed-system evolution over 125 ka should be ~1.10. Therefore, the theoretical expected value for the $(^{234}U/^{238}U)$ activity ratio measured in the S5 sapropel today is ~1.10. However, the measured $(^{234}U/^{238}U)$ activity ratios in the sapropel (Figure 2a) are markedly different from this expected value. The observed lower ratios close to the secular equilibrium in the center of the sapropel and the higher values (~1.15) at the top and base of the sapropel lead to apparent ages (calculated from the $^{234}U/^{238}U$ activity ratio assuming an initial $^{234}U/^{238}U$ ratio equal to 1.147) that are in strong contradiction with the known age of the S5 sapropel (125 ka) [*Lourens et al.*, 1996; *Löwemark et al.*, 2006]. It appears that the in situ formed radiogenic $^{234}U_{rad}$ diffuses preferentially away from the $^{238}U_{auth}$ peak, resulting in low and high $(^{234}U/^{238}U)$ activity ratios in the center and at the edges of the sapropel, respectively (Figure 2a) [*Mangini and Dominik*, 1979; *Severmann and Thomson*, 1998]. During alpha decay of $^{238}U_{auth}$, the recoil energy

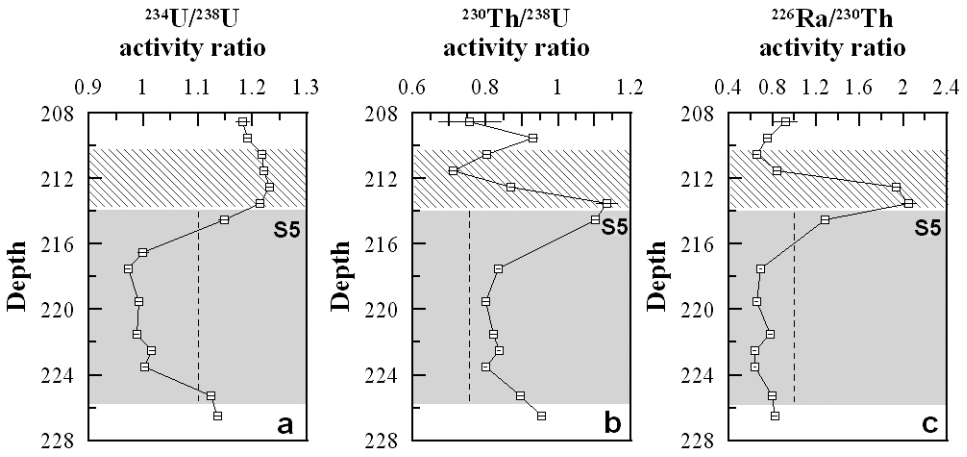

Figure 2. Depth variations in activity ratios through the Mn-rich zone (striped area) and the S5 sapropel (shaded area). The dashed lines represent the theoretical activity ratio values for the sapropel, assuming a seawater origin for U and a closed-system evolution with no initial ^{230}Th or ^{226}Ra. Error bars are included in the symbols and are expressed at a 95% confidence level.

given to the daughter ^{234}Th damages locally chemical bounding and is sufficient in many cases to cause the daughter ^{234}Th to be displaced from its lattice site to an interstitial location where it then rapidly decays, producing $^{234}U_{rad}$ [*Fleischer*, 1988]. This process makes $^{234}U_{rad}$ more reactive and prone to preferential diffusion relative to $^{238}U_{auth}$. The violation of the closed-system evolution of the S5 sapropel due to the preferential migration of $^{234}U_{rad}$ was the most important drawback for *Mangini and Dominik* [1979] and later *Severmann and Thomson* [1998] for obtaining the correct age of the S5 sapropel by employing the ^{230}Th/^{234}U disequilibrium dating method.

3.2.3. $^{230}Th_{xs}$ Versus U_{auth} Diffusion

[21] The (^{230}Th/^{238}U) activity ratio in the S5 sapropel is primarily controlled by the radioactive ingrowth of $^{230}Th_{auth}$ toward radioactive equilibrium with ^{234}U. The theoretical ^{230}Th/^{238}U activity ratio after 125 ka for a closed-system evolution of the ^{238}U chain, with an initial (^{234}U/^{238}U) activity ratio equal to 1.147, and without ^{230}Th initially present, is ~0.76. As can be seen from Figure 2b the measured (^{230}Th/^{238}U) activity ratios in the S5 sapropel are higher compared to the theoretical value. Considering that the detrital fraction does not significantly change the (^{230}Th/^{238}U) activity ratio, we propose two possible processes to explain this deviation.

3.2.3.1. $^{230}Th_{xs}$ Contribution in the S5 Sapropel

[22] An estimate of the $^{230}Th_{xs}$ fraction in the S5 sapropel, neglecting the detrital fraction, is given by the following equation:

$$^{230}Th_{xs} = \left[\left(\frac{^{230}Th}{^{238}U}\right)_{meas} - 0.76\right] \times {}^{238}U_{meas} \qquad (1)$$

where $^{238}U_{meas}$ and (^{230}Th/^{238}U)$_{meas}$ are the measured ^{238}U activity and (^{230}Th/^{238}U) activity ratio of the sapropel, respectively. The value 0.76 is the theoretical (^{230}Th/^{238}U) activity ratio for a closed-system evolution of the ^{238}U to ^{230}Th. The calculated $^{230}Th_{xs}$ values for the S5 sapropel are given in Table 2 (closed system). A relationship can be established between the calculated $^{230}Th_{xs}$ activity in the sapropel and the sedimentation rate S, assuming that during sapropel formation the flux of scavenged $^{230}Th_{xs}$ was equal to its production rate in the overlying water column:

$$S = \frac{P_{Th} \times Z}{DBD \times {}^{230}Th_{xs}} \times e^{-\lambda_{230} t} \qquad (2)$$

where P_{Th} is the production rate of ^{230}Th in seawater, Z is the sediment core water depth, DBD is the dry bulk density of the sapropel, λ_{230} the decay constant for the ^{230}Th, and t the time elapsed after $^{230}Th_{xs}$ deposition in the sapropel. An estimate of the sedimentation rate for the different $^{230}Th_{xs}$ activities of the S5 sapropel can be obtained from the equation 2, by using $P_{Th} = 2.67$ dpm cm^{-2} ka^{-1} km^{-1} [*Francois et al.*, 2004], $Z = 2.63$ km, an average dry

Table 2. Values of $^{230}Th_{xs}$, $^{231}Pa_{xs}$, and Age-Corrected $(^{231}Pa/^{230}Th)_{xs,o}$ for the S5 Sapropel[a]

Depth (cm)	$^{230}Th_{xs}$ (dpm/g)		$^{231}Pa_{xs}$ (dpm/g)	$(^{231}Pa/^{230}Th)_{xs,0}$	
	Closed System	Open System		Closed System	Open System
214.5	2.66 ± 0.08	2.11 ± 0.08			
217.5	3.52 ± 0.26	5.69 ± 0.26	0.051 ± 0.049	0.065 ± 0.063	0.040 ± 0.039
219.5	1.71 ± 0.46	3.14 ± 0.46	0.413 ± 0.048	1.084 ± 0.317	0.591 ± 0.110
221.5	2.70 ± 0.37	4.19 ± 0.37	0.625 ± 0.052	1.038 ± 0.167	0.668 ± 0.081
222.5	2.72 ± 0.19	3.84 ± 0.19			
223.5	1.74 ± 0.18	3.71 ± 0.18	0.101 ± 0.051	0.261 ± 0.134	0.122 ± 0.062
225.25	1.93 ± 0.15	0.99 ± 0.15			

[a]The $^{230}Th_{xs}$ and, by consequence, the $(^{231}Pa/^{230}Th)_{xs,0}$ ratios are calculated by considering a closed-system evolution of the sapropel ("Closed System" entries) and with the model ("Open System" entries) that takes into account the impact of $^{234}U_{rad}$ diffusion on $^{230}Th_{auth}$ formation. For age correction all sapropel samples are assumed to be the same age (125 ka). Errors are expressed at a 95% confidence level.

bulk density for the sapropel of about 1 g cm^{-3} [*Diester-Haass et al.*, 1998; *Nijenhuis et al.*, 2001], $\lambda_{230} = 9.16 \times 10^{-3}$ ka^{-1}, and $t = 125$ ka as an average age for the S5. The estimated sedimentation rate during S5 sapropel formation varies between 0.6 and 1.3 cm ka^{-1} (Figure 3). This range of sedimentation rates during S5 sapropel formation appears low compared to what would be expected from previous studies. Considering that the average sedimentation rate of the eastern Mediterranean Sea is of about 2 cm ka^{-1} [*Murat and Got*, 1989] and that S5 sapropel corresponds to an episode of increasing input of freshwater and high primary productivity [*Emeis and Sakamoto*, 1998; *Löwemark et al.*, 2006; *Osborne et al.*, 2010; *Rohling et al.*, 2006; *Weldeab et al.*, 2003], the estimated sedimentation rate for the S5 sapropel should not be less than 2 cm ka^{-1}. This underestimation of the sedimentation rate can probably be explained by a disturbance of the balance between the flux of $^{230}Th_{xs}$ scavenged from the water column and its rate of production. The underlying assumption that the flux of $^{230}Th_{xs}$ scavenged to the seafloor was exactly equal to its rate of production in the overlying water during S5 sapropel formation might not be valid under conditions where there is a large vertical particle flux. There is a process known as 'boundary scavenging' [*Spencer et al.*, 1981] in which a somewhat higher flux of $^{230}Th_{xs}$ relative to its production rate is observed in regions of high particle flux. As can be seen from the equation 2 a somewhat higher flux of $^{230}Th_{xs}$ than the production rate should underestimate the sedimentation rate of the sapropel. However, the very short residence time of $^{230}Th_{xs}$ (10–50 years) in seawater indicates that the processes that can disturb the balance between the flux of $^{230}Th_{xs}$ and its rate of production must be limited and thus the flux of $^{230}Th_{xs}$ should always be close to its rate of production [*Anderson et al.*, 1990].

3.2.3.2. Diffusion of U_{auth}

[23] The diffusion of U_{auth} in the center of the sapropel unit might be an alternative process that could explain the observed high $(^{230}Th/^{238}U)$ activity ratio. Considering that ^{230}Th is immobile due to its high particle reactivity, diffusion of U_{auth} away from the U concentration peak in the center of the sapropel would result in a higher $(^{230}Th/^{238}U)$ ratio compared with the expected value assuming a closed-system evolution. Although U(IV) is considered geochemically immobile, the occurrence of

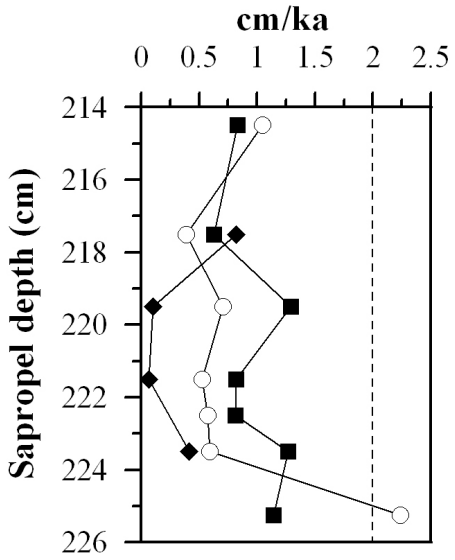

Figure 3. Estimated sedimentation rates for the S5 sapropel, calculated using three different methods (see text for details): (1) using the calculated $^{230}Th_{xs}$ for a closed-system evolution with no $^{234}U_{rad}$ migration (squares), (2) by taking into account the $^{234}U_{rad}$ migration (open dots), and (3) by using the $^{231}Pa_{xs}$ (diamonds). The dashed line represents the average sedimentation rate for the eastern Mediterranean Sea [*Murat and Got*, 1989].

high dissolved U concentrations in pore waters of anoxic sediments has already been reported [*Anderson et al.*, 1989b; *Chaillou et al.*, 2002; *Cochran et al.*, 1986]. In most cases the authors attributed this presence to air contamination during the process of sampling the pore waters that induced reoxidation of U(IV) to soluble U(VI). However, oxidation of U(IV) to U(VI) by nitrogen species under anoxic conditions [*Finneran et al.*, 2002], and the production of authigenic colloidal U(IV) by microbial remediation, has also been demonstrated [*Fredrickson et al.*, 2000]. In our case, gamma measurement of ^{234}Th in one sample from the sapropel, two days after opening of the core in the laboratory, was found to be in secular equilibrium with ^{238}U measured by TIMS. We believe that, even if U has been oxidized after the core opening it should not diffuse in the sapropel. Therefore, we propose that if U_{auth} diffusion in the sapropel occurred, it would have been a continuous process over the last 125 ka since the sapropel formation. However, the remaining $^{230}Th_{xs}$ in the sapropel and the poorly understood processes favoring U diffusion in anoxic sediments make U_{auth} diffusion in the sapropel unclear.

3.2.4. Is Diffusion Process in S5 Sapropel Still Active?

[24] The (^{226}Ra/^{230}Th) activity ratio can be used as a tool for investigating if migration of radionuclides in the S5 sapropel was continuously active up until the present day or if it was inhibited several thousand of years after S5 sapropel deposition by processes like sediment compaction. It is well known that the ^{226}Ra nuclide has a high mobility in pore waters of near surface sediments [*Cochran*, 1980; *Cochran and Krishnaswami*, 1980; *Ku*, 1965] and in organic-rich turbidites [*Colley and Thomson*, 1992]. Considering that ^{230}Th in sediments is immobile and that the half-life of ^{226}Ra is just 1.6 ka, the return to secular equilibrium of (^{226}Ra/^{230}Th) activity ratio after a system disturbance (gain or loss of ^{226}Ra) is rapid (≤9.6 ka). Therefore, disequilibrium between ^{226}Ra and ^{230}Th in the S5 sapropel indicates the active migration of ^{226}Ra (and probably of $^{234}U_{rad}$) since the last 115 ka. Indeed, as can be seen from the Figure 2c ^{226}Ra shows clear evidence of diffusion in the S5 sapropel. Diffusion of ^{226}Ra away from ^{230}Th peak emphasizes the (^{226}Ra/^{230}Th) ratio depletion at the ^{230}Th peak. On the contrary, excess of ^{226}Ra is observed only in the top of the sapropel unit showing probably a preferential upwards migration of ^{226}Ra (Figure 2c).

3.2.5. Mn-Rich Zone: Evidence for Outward Nuclide Diffusion From the Sapropel

[25] Bottom water reoxygenation after sapropel formation generated a progressive downward migrating oxidation front that has burnt down the high C_{org} contents of the top of the S5 sapropel. When the oxidation front meets the dissolved Mn(II) in the sapropel pore water that is used as a terminal electron acceptor, Mn precipitates forming a Mn-oxide peak (Mn-rich zone). For this reason C_{org} content is very low in the Mn-rich zone and sharply increases at the upper edge of the S5 sapropel (Figure 1a).

[26] This phenomenon has been intensely studied for the most recent S1 sapropel [*De Lange et al.*, 1999; *Jung et al.*, 1997; *Mercone et al.*, 2001; *ten Haven et al.*, 1988; *Thomson et al.*, 1999].

[27] During the early stages of sapropel burn-down significant amounts of U_{auth} is released to pore water and diffuses along the concentration gradient. Part of the dissolved U diffuses back into the ocean and in many cases a downward migration and redeposition of U below the oxidation front has been observed [*Colley et al.*, 1989; *Mangini et al.*, 2001]. Here, small but significant ^{234}U and ^{238}U peaks were observed in the Mn-rich zone (Figure 1b). We believe that after oxidation a part of the mobilized U coprecipitates with Mn-oxides (due to the high U affinities with Mn) forming a characteristic U peak in the Mn-rich zone. Therefore, U in the Mn-rich zone is a mixture of U_{det} and U_{auth} with a $(^{234}U/^{238}U)_{det}$ ratio ≤1 and a $(^{234}U/^{238}U)_{auth}$ ratio after 125 ka equal to ~1.10. The high (^{234}U/^{238}U) activity ratios (>1.2) observed in the Mn-rich zone (Figure 2a) clearly point toward a continuous outward $^{234}U_{rad}$ diffusion from the sapropel and fixation in the Mn-rich zone. We should point out that pelagic sediments generate $^{234}U_{rad}$ in the pore waters as well, but here we consider that the sapropel with high uranium contents is at the origin of $^{234}U_{rad}$ in the pore waters.

[28] High variations of the (^{230}Th/^{238}U) activity ratio in the Mn-rich zone are observed (Figure 2b). Theses variations could be explained by the low $^{230}Th_{auth}$ in situ produced by U_{auth} decay and the high $^{230}Th_{det}$ and $^{230}Th_{xs}$ contributions.

[29] A small but significant ^{226}Ra peak is also observed at the bottom of the Mn-rich zone (Figure 1b). Higher ^{226}Ra affinities for Mn than U might be probably the reason for U and ^{226}Ra decoupled peaks (Figure 1b). The high ^{226}Ra excess

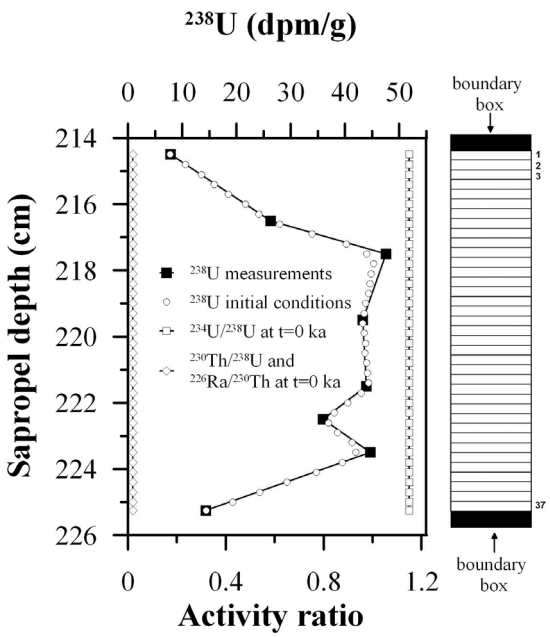

Figure 4. The model ^{238}U initial conditions derived from the ^{238}U measured profile and the initial (^{234}U/^{238}U), (^{230}Th/^{238}U) and (^{226}Ra/^{230}Th) activity ratios. The outermost black areas represent the boundary boxes used in the model.

at the bottom of the Mn-rich zone (Figure 2c) shows clear evidence of continuous diffusion of ^{226}Ra out of the sapropel and fixation in the Mn-rich zone. Thus we believe that continuous supply of ^{226}Ra originating form the sapropel dominates ^{226}Ra loss by radioactive decay maintaining the high (^{226}Ra/^{230}Th) activity ratios in the bottom of the Mn-rich zone.

3.3. Estimation of Diffusion Coefficients

3.3.1. One-Dimensional Diffusion Box Model

[30] In order to test the influence of nuclide diffusion on (^{234}U/^{238}U), (^{230}Th/^{238}U) and (^{226}Ra/^{230}Th) ratios for S5 sapropel, a simple 1-D diffusion box model was developed. By tuning the model to generate activity ratio profiles that match the observed profiles, an estimate of the diffusion coefficients was made. The processes that are modeled are diffusion of ^{234}U$_{rad}$ and ^{226}Ra and radioactive decay of the ^{238}U → ^{234}U → ^{230}Th → ^{226}Ra chain. ^{230}Th is considered as immobile due to its high particle reactivity. The intermediate daughter radionuclides of the decay chain may be ignored because their half-lives are too short to consider significant diffusion from the production site. The model system equation follows the next form:

$$\frac{dN^i_{238}}{dt} = -\lambda_{238}N^i_{238} \tag{3}$$

$$\frac{dN^i_{234}}{dt} = -\lambda_{234}N^i_{234} \tag{4}$$

$$\frac{dN^{rad(i)}_{234}}{dt} = \lambda_{238}N^i_{238} - \lambda_{234}N^{rad(i)}_{234} + D_{rad}\frac{\partial^2 N^{rad}_{234}}{\partial z^2} \tag{5}$$

$$\frac{dN^i_{230}}{dt} = \lambda_{234}N^i_{234} + \lambda_{234}N^{rad(i)}_{234} - \lambda_{230}N^i_{230} \tag{6}$$

$$\frac{dN^i_{226}}{dt} = \lambda_{230}N^i_{230} - \lambda_{226}N^i_{226} + D_{Ra}\frac{\partial^2 N_{226}}{\partial z^2} \tag{7}$$

where N^i_{238}, N^i_{234}, $N^{rad(i)}_{234}$, N^i_{230}, N^i_{226} are the number of nuclides for box «*i*» of $^{238}U_{auth}$, $^{234}U_{auth}$, $^{234}U_{rad}$, ^{230}Th and ^{226}Ra, respectively; λ_{238}, λ_{234}, λ_{230}, λ_{226} are the radioactive decay constants for ^{238}U, ^{234}U, ^{230}Th and ^{226}Ra respectively; and t is the time before present since S5 formation (i.e., 125 ka). D_{rad} and D_{Ra} are the diffusion coefficients for ^{234}U$_{rad}$ and ^{226}Ra, respectively. As can be seen from the equation 5, radiogenic ^{234}U$_{rad}$ is considered separately as in the approach of *Robinson et al.* [2006], who tried to model diffusion of ^{234}U$_{rad}$ in deep water corals. The initial conditions of the model are derived by dividing the ^{238}U measured profile in 37 parallel boxes of 3.1 mm width and using the ^{238}U activities of the center of the boxes (Figure 4).

[31] In addition to ^{238}U initial activities, the initial (^{234}U/^{238}U) ratio in the sapropel is considered to be equal to the modern seawater value of 1.147 and no initial ^{230}Th and ^{226}Ra are present (^{230}Th/^{238}U = ^{226}Ra/^{230}Th = 0) (Figure 4). We should point out that for the initial model conditions we consider that the oxidation of the upper edge of the sapropel, that can modify the shape of the ^{238}U profile, is a rapid phenomenon compared to the age of the S5 sapropel. For the model boundary conditions a low ^{238}U activity of about 2 dpm g^{-1} is used and the radioactive chain ^{238}U → ^{234}U → ^{230}Th → ^{226}Ra is considered to be in secular equilibrium. The best fit of the model is assessed by minimizing the Sums of Squares of Differences (SSD) between the model output and measured activity ratios. The fit error typically of about 15% is given as the uncertainty in the diffusion coefficients.

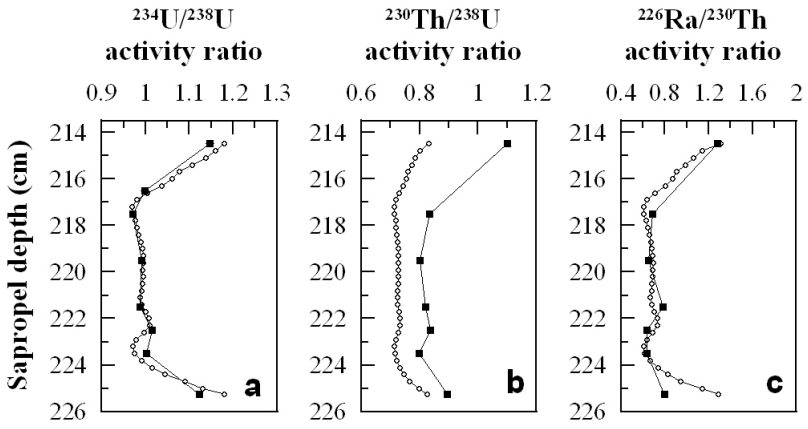

Figure 5. Best fit model (open dots) for the ($^{234}U/^{238}U$), ($^{230}Th/^{238}U$) and ($^{226}Ra/^{230}Th$) activity ratio profiles (squares) through the S5 sapropel.

3.3.2. $^{234}U_{rad}$, ^{226}Ra Diffusion Coefficients and $^{230}Th_{xs}$ Revaluation

[32] The model allows running processes of radioactive decay and diffusion for 125 ka. The best fit for the ($^{234}U/^{238}U$) ratio is obtained for a diffusion coefficient D_{rad} of about $(7.1 \pm 1.1) \times 10^{-12}$ cm^2 s^{-1} (Figure 5a). This value is in a good agreement with the diffusion coefficient reported by *Mangini and Dominik* [1979] who propose a D_{rad} value for a S5 sapropel varying between 10^{-11} and 10^{-12} cm^2 s^{-1}. Other scientific works have reported higher D_{rad} values ($1–4.5 \times 10^{-8}$ cm^2 s^{-1}) from a variety of sediment types [*Henderson et al.*, 1999b; *Ku*, 1965]. In organic-rich turbidites of Madeira Abyssal Plain a good chemical closure in the $^{238}U \rightarrow ^{230}Th$ decay sequence has reported with D_{rad} diffusion coefficients $<10^{-15} – 10^{-14}$ cm^2 s^{-1} [*Colley and Thomson*, 1990; *Colley and Thomson*, 1992]. The $D_{rad} \sim 7 \times 10^{-12}$ cm^2 s^{-1} found for the S5 sapropel is 10^5–10^6 times lower than for conservative species in marine sediments [*Li and Gregory*, 1974]. This suggests that prevailing reducing conditions in sapropels or turbidites are probably the cause of the apparent retardation of the diffusion of $^{234}U_{rad}$ atoms.

[33] Based on our best estimate of D_{rad}, the model allows calculation of the ($^{230}Th/^{238}U$) ratio taking into account the impact of the $^{234}U_{rad}$ diffusion on the ^{230}Th radioactive ingrowth toward ^{238}U. As can be seen from Figure 5b, the modeled ($^{230}Th/^{238}U$) profile is systematically lower than the measured one. This model deviation from the experimental data can be explained by the contribution of $^{230}Th_{xs}$ initially present in the sapropel. Therefore, a simple subtraction of modeled and measured ($^{230}Th/^{238}U$) ratios can be used for the recalculation of the $^{230}Th_{xs}$ (Table 2). This approach for $^{230}Th_{xs}$ calculation seems more realistic because the theoretical value of 0.76 that was used in the section 3.2.3 for calculating $^{230}Th_{xs}$ is for a closed-system evolution (without $^{234}U_{rad}$ diffusion).

[34] From the recalculated $^{230}Th_{xs}$ and by using the equation 2 a revaluation of the sedimentation rate during S5 sapropel formation can be made. The revaluated sedimentation rate for the center of the sapropel unit is even lower compared to the sedimentation rate calculated in the section 3.2.3 and equals to ~0.5 cm ka^{-1} (Figure 3, open dots). This lower average sedimentation rate boost the discordance between the mechanisms of S5 sapropel formation that have been advanced and the estimated sedimentation rate from $^{230}Th_{xs}$ in this work. This discordance, as mentioned above, involves a disturbance of the seawater $^{230}Th_{xs}$ flux during sapropel formation and/or U_{auth} diffusion.

[35] A new version of the model taking into account not only the $^{234}U_{rad}$ diffusion but also the diffusion of the U_{auth} should be a good approach to test the impact of the U_{auth} diffusion on the ($^{230}Th/^{238}U$) ratio. However, one major drawback for testing U_{auth} diffusion is lack of knowledge on the initial U conditions because continuous U_{auth} diffusion inhibits the use of the measured profile as initial conditions.

[36] The best fit for the ($^{226}Ra/^{230}Th$) ratio between the modeled and the measured profiles is obtained for a diffusion coefficient D_{Ra} of about $(1.6 \pm 0.2) \times 10^{-10}$cm^2 s^{-1} (Figure 5c). This value is comparable to the diffusion coefficient reported by *Colley and Thomson* [1992] ($D_{Ra} \sim 7 \times 10^{-10}$ cm^2 s^{-1}) for deep

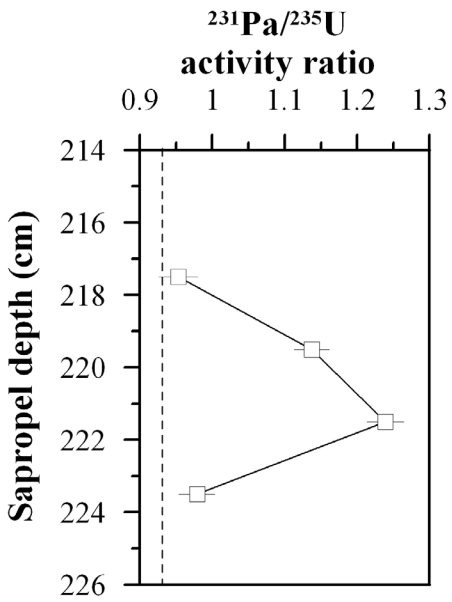

Figure 6. (^{231}Pa/^{235}U) activity ratio profile through the S5 sapropel. The dashed line represents the theoretical activity ratio, assuming a closed-system evolution for the sapropel with no initial ^{231}Pa. Error bars are expressed at a 95% confidence level.

sea turbidites with the presumption that 100% of ^{226}Ra is mobile. The model poor precision for the lower edge of the sapropel is probably due to a preferential upward diffusion of ^{226}Ra that has not been taken into account in the model.

3.4. ^{235}U Decay Chain as an Alternative Dating Tool

[37] In order to avoid system closure problems due to $^{234}U_{rad}$ migration the ^{235}U decay chain was studied. The $^{235}U \rightarrow {}^{231}Th \rightarrow {}^{231}Pa$ chain is independent of the mobility of radiogenic $^{234}U_{rad}$ and geochemistry of ^{231}Pa (32.76 ka) is similar to that of ^{230}Th showing high affinities with particle surfaces and thus can be considered as immobile. The intermediate ^{231}Th nuclide can be ignored because of its very short half-life (25.5h). Therefore, the radioactive ingrowth of ^{231}Pa toward ^{235}U can be used as an alternative dating tool for the S5 sapropel.

[38] Like ^{230}Th and ^{226}Ra three distinct sources have also to be distinguished for sedimentary ^{231}Pa: (1) detrital $^{231}Pa_{det}$ locked in the mineral lattices and which is considered in secular equilibrium with $^{235}U_{det}$, (2) authigenic $^{231}Pa_{auth}$ produced in the sediments from the radioactive decay of the seawater derived $^{235}U_{auth}$, and (3) $^{231}Pa_{xs}$ scavenged from the water column by adsorption on the settling particles.

[39] As stated in the section 3.2.1., due to low ^{232}Th activities in sapropel compared with the high U activities, the detrital fraction can be neglected. The relative difference between the uncorrected and the detrital-free (^{231}Pa/^{235}U) ratio varies between 0.01% and 0.3% which is smaller than the analytical uncertainty (~2%).

[40] For ^{231}Pa analyses four samples from the center of the sapropel with high ^{238}U activities and similar (^{234}U/^{238}U) ratios were selected. Considering a closed-system evolution for the sapropel without initial ^{231}Pa present and for 125 ka elapsed after system closure the theoretical (^{231}Pa/^{235}U) activity ratio must be equal to 0.93. As can be seen from the Figure 6 the measured (^{231}Pa/^{235}U) ratios in the center of the sapropel unit are surprisingly higher compared to the expected theoretical value. Thus, the $^{231}Pa_{xs}$ contribution in the sapropel was investigated as a potential explanation for the high (^{231}Pa/^{235}U) ratios. An estimate of the $^{231}Pa_{xs}$ for the S5 sapropel is provided by using the following equation:

$$^{231}Pa_{xs} = \left[\left(\frac{^{231}Pa}{^{235}U}\right)_{meas} - 0.93\right] \times \frac{^{238}U_{meas}}{21.72} \qquad (8)$$

where (^{231}Pa/^{235}U)$_{meas}$ is the measured (^{231}Pa/^{235}U) ratio and $^{238}U_{meas}$ is the measured ^{238}U activity. The calculated values of the $^{231}Pa_{xs}$ are given the Table 2. The ^{231}Pa production rate in the seawater can be calculated according to equation (9):

$$P_{Pa} = 0.115 \text{ dpm } l^{-1} \times 2.11 \times 10^{-2} \text{ ka}^{-1} \times 100 \text{ l cm}^{-2} \text{ km}^{-1}$$
$$= 0.243 \text{ dpm cm}^{-2} \text{ km}^{-1} \text{ ka}^{-1} \qquad (9)$$

where 0.115 dpm l^{-1} is the seawater ^{235}U activity for a salinity of 35 ‰ [*Pates and Muir*, 2007], 2.11 × 10^{-2} ka^{-1} is the decay constant of ^{231}Pa and, 100 l cm^{-2} km^{-1} is the volume of water per km height over an area of 1 cm^2.

[41] Assuming that during S5 sapropel formation the flux of scavenged $^{231}Pa_{xs}$ was equal to its production rate in the water column, the equation 2 can be rewritten for ^{231}Pa allowing the evaluation of the sedimentation rate. As can be seen from the Figure 3 (diamonds), the high $^{231}Pa_{xs}$ values lead to unrealistic low sedimentation rates for the center of the S5 sapropel. We calculated, the (^{231}Pa/^{230}Th) excess corrected to the time of deposition in the sediment ((^{231}Pa/^{230}Th)$_{xs,0}$) to infer any effect of boundary scavenging on ^{230}Th and ^{231}Pa during the deposition of the sapropel [*Bacon*, 1988; *Francois et al.*, 2007]. This ratio was calculated (1) considering a closed-system evolution for the $^{230}Th_{xs}$ and (2) by taking

into account the $^{234}U_{rad}$ diffusion (open system). As can be seen from Table 2, the $(^{231}Pa/^{230}Th)_{xs,0}$ values for the open system are significantly lower compared with the values of the closed system. The open-system approach for calculating the $(^{231}Pa/^{230}Th)_{xs,0}$ seems to be more realistic because of $^{234}U_{rad}$ diffusion that has been taken into account in the $^{230}Th_{xs}$ calculation.

[42] At present, there are no similar data for the modern Mediterranean Sea for comparison. For the samples 217.5 and 225.25 the high uncertainty on the $(^{231}Pa/^{230}Th)_{xs,0}$ values does not allow a satisfactory interpretation. However, it seems that the $(^{231}Pa/^{230}Th)_{xs,0}$ values of samples 219.5 and 221.5 are unrealistically high for both open- and closed-system calculations. Such high ratios have never been found, even in high productivity, high opal flux regions such as the Southern Ocean [*Anderson et al.*, 2009; *Walter et al.*, 1997] or the Equatorial Pacific [*Bradtmiller et al.*, 2006; *Pichat et al.*, 2004]. Although we cannot completely rule out the possibility of enhanced boundary scavenging during sapropel formation, these unrealistically high $(^{231}Pa/^{230}Th)_{xs,0}$ ratios call probably for other processes like a combination of U_{auth} diffusion over the time and an enhanced boundary scavenging during sapropel formation. The study of well-preserved sapropels older than S5 (e.g., S7–S11) in which the $^{230}Th_{xs}$ and $^{231}Pa_{xs}$ has completely decayed away, might provide a more suitable case for investigating U_{auth} migration processes.

4. Conclusion

[43] This work provides isotopic measurements of the U decay series across a ~125 ka S5 sapropel layer from the Mediterranean Sea, using more precise mass spectrometric methods (TIMS/MC-ICPMS) and high-efficiency low-background gamma spectrometry. The exceptionally high organic carbon concentration of the S5 sapropel limits postdepositional oxidation and makes this sapropel among one of the best preserved. Deviation of the $(^{234}U/^{238}U)$ activity ratio from the theoretical value, assuming a seawater U origin and a closed-system evolution, confirms $^{234}U_{rad}$ migration away from the U peak in the center of the sapropel. In addition, the fact that ^{226}Ra with a short half-life is not in secular equilibrium with ^{230}Th, shows that migration of ^{226}Ra (and probably of $^{234}U_{rad}$) is a quasi-continuous process acting since the formation of S5. Apparently this migration is not limited to the inside of the sapropel. High $(^{234}U/^{238}U)$ and $(^{226}Ra/^{230}Th)$ activity ratios in the overlying Mn-rich zone show evidence of nuclide migration out of the sapropel. In order to constrain diffusion coefficients for $^{234}U_{rad}$ and ^{226}Ra a simple 1-D diffusion model was developed. The best fit between the model output and the measured $(^{234}U/^{238}U)$, $(^{226}Ra/^{230}Th)$ profiles was obtained for D_{rad} and D_{Ra} equal to $(7.1 \pm 1.1) \times 10^{-12}$ cm^2 s^{-1} and $(1.6 \pm 0.2) \times 10^{-10}$ cm^2 s^{-1}, respectively. However, $^{234}U_{rad}$ diffusion cannot explain the high $(^{230}Th/^{238}U)$ activity ratio values observed in the sapropel. Two possible mechanisms or a combination of both of them are proposed for explaining the irregular $(^{230}Th/^{238}U)$ activity profile in the S5 sapropel. The first one is an important flux of $^{230}Th_{xs}$ higher than its production rate in the water column during sapropel formation and the second one is diffusion of U_{auth} in the sapropel. We believe that, if U_{auth} diffusion in the sapropel exists, the scenario of U diffusion after the core opening seems unlikely because ^{234}Th was found to be in secular equilibrium with ^{238}U two days after the core opening. It was hoped that the use of the $(^{231}Pa/^{235}U)$ ratio might be an alternative dating tool for the sapropel S5. Unfortunately, surprisingly high $(^{231}Pa/^{235}U)$ activity ratios compared to the theoretical value are observed in the center of the S5 sapropel. A high $^{231}Pa_{xs}$ flux during sapropel formation and/or U_{auth} migration is proposed in order to explain the high $(^{231}Pa/^{235}U)$ activity ratios. The study of sapropels older than S5, in which the $^{230}Th_{xs}$ and $^{231}Pa_{xs}$ has completely decayed away, should provide a better example to investigate U_{auth} migration processes.

Acknowledgments

[44] The authors warmly thank A. Mangini, A. Thomas, D. Peate, S. Severmann and Y. Zheng for their constructive comments that profoundly improved this paper. We would like also to thank E. Robin for Mn measurements.

References

Aksu, A. E., D. Yasar, and P. J. Mudie (1995), Paleoclimatic and paleoceanographic conditions leading to development of sapropel layer Sl in the Aegean Sea, *Palaeogeogr. Palaeoclimatol. Palaeoecol.*, *116*(1–2), 71–101, doi:10.1016/0031-0182(94)00092-M.

Andersen, M. B., C. H. Stirling, B. Zimmermann, and A. N. Halliday (2010), Precise determination of the open ocean $^{234}U/^{238}U$ composition, *Geochem. Geophys. Geosyst.*, *11*, Q12003, doi:10.1029/2010GC003318.

Anderson, R. F., M. Q. Fleisher, and A. P. LeHuray (1989a), Concentration, oxidation state, and particulate flux of uranium in the Black Sea, *Geochim. Cosmochim. Acta*, *53*(9), 2215–2224, doi:10.1016/0016-7037(89)90345-1.

Anderson, R. F., A. P. Lehuray, M. Q. Fleisher, and J. W. Murray (1989b), Uranium deposition in Saanich Inlet sediments, Vancouver Island, *Geochim. Cosmochim. Acta*, *53*(9), 2205–2213, doi:10.1016/0016-7037(89)90344-X.

Anderson, R. F., Y. Lao, W. S. Broecker, S. E. Trumbore, H. J. Hofmann, and W. Wolfli (1990), Boundary scavenging in the Pacific Ocean: A comparison of ^{10}Be and ^{231}Pa, *Earth Planet. Sci. Lett.*, *96*(3–4), 287–304, doi:10.1016/0012-821X(90)90008-L.

Anderson, R. F., S. Ali, L. I. Bradtmiller, S. H. H. Nielsen, M. Q. Fleisher, B. E. Anderson, and L. H. Burckle (2009), Wind-driven upwelling in the Southern Ocean and the deglacial rise in atmospheric CO_2, *Science*, *323*(5920), 1443–1448, doi:10.1126/science.1167441.

Bacon, M. P. (1988), Tracers of chemical scavenging in the ocean—Boundary effects and large-scale chemical fractionation, *Philos. Trans. R. Soc. London, Ser. A*, *325*(1583), 147–160.

Barnes, C. E., and J. K. Cochran (1990), Uranium removal in oceanic sediments and the oceanic U balance, *Earth Planet. Sci. Lett.*, *97*(1–2), 94–101, doi:10.1016/0012-821X(90)90101-3.

Barnes, E. C., and J. K. Cochran (1991), Geochemistry of uranium in Black Sea sediments, *Deep Sea Res. Part A*, *38*, S1237–S1254, doi:10.1016/S0198-0149(10)80032-9.

Bernat, M., A. Buscail, A. Monaco, H. Got, and B. Chassefiere (1989), Concentrations en uranium et desequilibres radioactifs Io–U en Mediterranee orientale—Discussion sur l'origine des sapropeles, *Chem. Geol.*, *75*(4), 329–337, doi:10.1016/0009-2541(89)90005-3.

Bishop, J. K. B. (1988), The barite-opal-organic carbon association in oceanic particulate matter, *Nature*, *332*(6162), 341–343, doi:10.1038/332341a0.

Bradtmiller, L. I., R. F. Anderson, M. Q. Fleisher, and L. H. Burckle (2006), Diatom productivity in the equatorial Pacific Ocean from the last glacial period to the present: A test of the silicic acid leakage hypothesis, *Paleoceanography*, *21*, PA4201, doi:10.1029/2006PA001282.

Castradori, D. (1993), Calcareous nannofossils and the origin of the eastern Mediterranean sapropels, *Paleoceanography*, *8*(4), 459–471, doi:10.1029/93PA00756.

Chaillou, G., P. Anschutz, G. Lavaux, J. Schafer, and G. Blanc (2002), The distribution of Mo, U, and Cd in relation to major redox species in muddy sediments of the Bay of Biscay, *Mar. Chem.*, *80*(1), 41–59, doi:10.1016/S0304-4203(02)00097-X.

Chen, J. H., R. L. Edwards, and G. J. Wasserburg (1986), ^{238}U, ^{234}U and ^{232}Th in seawater, *Earth Planet. Sci. Lett.*, *80*, 241–251, doi:10.1016/0012-821X(86)90108-1.

Cheng, H., R. L. Edwards, J. Hoff, C. D. Gallup, D. A. Richards, and Y. Asmerom (2000), The half-lives of uranium-234 and thorium-230, *Chem. Geol.*, *169*, 17–33, doi:10.1016/S0009-2541(99)00157-6.

Cita, M. B., C. Vergnaud-Grazzini, C. Robert, H. Chamley, N. Ciaranfi, and S. Donofrio (1977), Paleoclimatic record of a long deep sea core from the eastern Mediterranean, *Quat. Res.*, *8*(2), 205–235, doi:10.1016/0033-5894(77)90046-1.

Cochran, J. K. (1980), The flux of ^{226}Ra from deep-sea sediments, *Earth Planet. Sci. Lett.*, *49*(2), 381–392, doi:10.1016/0012-821X(80)90080-1.

Cochran, J. K., and S. Krishnaswami (1980), Radium, thorium, uranium, and ^{210}Pb in deep-sea sediments and sediment pore waters from the north equatorial Pacific, *Am. J. Sci.*, *280*(9), 849–889, doi:10.2475/ajs.280.9.849.

Cochran, J. K., A. E. Carey, E. R. Sholkovitz, and L. D. Surprenant (1986), The geochemistry of uranium and thorium in coastal marine sediments and sediment pore waters, *Geochim. Cosmochim. Acta*, *50*(5), 663–680, doi:10.1016/0016-7037(86)90344-3.

Colley, S., and J. Thomson (1990), Limited diffusion of U-series radionuclides at depth in deep-sea sediments, *Nature*, *346*(6281), 260–263, doi:10.1038/346260a0.

Colley, S., and J. Thomson (1992), Behaviour and mobility of U series radionuclides in Madeira Abyssal Plain turbidites over the past 750,000 years, *Mar. Geol.*, *109*(1–2), 141–158, doi:10.1016/0025-3227(92)90225-7.

Colley, S., J. Thomson, and J. Toole (1989), Uranium relocations and derivation of quasi-isochrons for a turbidite/pelagic sequence in the northeast Atlantic, *Geochim. Cosmochim. Acta*, *53*(6), 1223–1234, doi:10.1016/0016-7037(89)90058-6.

De Lange, G. J., and H. L. ten Haven (1983), Recent Sapropel Formation in the Eastern Mediterranean, *Nature*, *305*(5937), 797–798, doi:10.1038/305797a0.

De Lange, G. J., P. J. M. Van Santvoort, C. Langereis, J. Thomson, C. Corselli, A. Michard, M. Rossignol-Strick, M. Paterne, and G. Anastasakis (1999), Palaeo-environmental variations in eastern Mediterranean sediments: A multidisciplinary approach in a prehistoric setting, *Prog. Oceanogr.*, *44*(1–3), 369–386, doi:10.1016/S0079-6611(99)00037-3.

Diester-Haass, L., C. Robert, and H. Chamley (1998), Paleoproductivity and climate variations during sapropel deposition in the eastern Mediterranean Sea, *Proc. Ocean Drill. Program Sci. Results*, *160*, 227–247.

Emeis, K.-C., and T. Sakamoto (1998), The sapropel theme of Leg 160, *Proc. Ocean Drill. Program Sci. Results*, *160*, 29–36.

Emeis, K.-C., T. Sakamoto, R. Wehausen, and H.-J. Brumsack (2000a), The sapropel record of the eastern Mediterranean Sea—Results of Ocean Drilling Program Leg 160, *Palaeogeogr. Palaeoclimatol. Palaeoecol.*, *158*(3–4), 371–395, doi:10.1016/S0031-0182(00)00059-6.

Emeis, K.-C., U. Struck, H.-M. Schulz, R. Rosenberg, S. Bernasconi, H. Erlenkeuser, T. Sakamoto, and F. Martinez-Ruiz (2000b), Temperature and salinity variations of Mediterranean Sea surface waters over the last 16,000 years from records of planktonic stable oxygen isotopes and alkenone unsaturation ratios, *Palaeogeogr. Palaeoclimatol. Palaeoecol.*, *158*(3–4), 259–280, doi:10.1016/S0031-0182(00)00053-5.

Finneran, K. T., R. T. Anderson, K. P. Nevin, and D. R. Lovley (2002), Potential for bioremediation of uranium-contaminated aquifers with microbial U(VI) reduction, *Soil Sediment Contam.*, *11*(3), 339–357, doi:10.1080/20025891106781.

Fleischer, R. L. (1988), Alpha-recoil damage: Relation to isotopic disequilibrium and leaching of radionuclides, *Geochim. Cosmochim. Acta*, *52*(6), 1459–1466, doi:10.1016/0016-7037(88)90216-5.

Francois, R., M. Frank, M. M. Rutgers van der Loeff, and M. P. Bacon (2004), ^{230}Th normalization: An essential tool for interpreting sedimentary fluxes during the late Quaternary, *Paleoceanography*, *19*, PA1018, doi:10.1029/2003PA000939.

Francois, R., et al. (2007), Comment on "Do geochemical estimates of sediment focusing pass the sediment test in the equatorial Pacific?" by M. Lyle et al, *Paleoceanography*, *22*, PA1216, doi:10.1029/2005PA001235.

Fredrickson, J. K., J. M. Zachara, D. W. Kennedy, M. C. Duff, Y. A. Gorby, S. M. W. Li, and K. M. Krupka (2000), Reduction of U(VI) in goethite (alpha-FeOOH) suspensions by a

dissimilatory metal-reducing bacterium, *Geochim. Cosmochim. Acta*, *64*(18), 3085–3098, doi:10.1016/S0016-7037(00)00397-5.

Guihou, A., S. Pichat, S. Nave, A. Govin, L. Labeyrie, E. Michel, and C. Waelbroeck (2010), Late slowdown of the Atlantic Meridional Overturning Circulation during the Last Glacial Inception: New constraints from sedimentary (^{231}Pa/^{230}Th), *Earth Planet. Sci. Lett.*, *289*(3–4), 520–529, doi:10.1016/j.epsl.2009.11.045.

Henderson, G. M. (2002), Seawater (^{234}U/^{238}U) during the last 800 thousand years, *Earth Planet. Sci. Lett.*, *199*(1–2), 97–110, doi:10.1016/S0012-821X(02)00556-3.

Henderson, G. M., and R. F. Anderson (2003), The U-series toolbox for paleoceanography, *Rev. Mineral. Geochem.*, *52*(1), 493–531, doi:10.2113/0520493.

Henderson, G. M., C. Heinze, R. F. Anderson, and A. M. E. Winguth (1999a), Global distribution of the ^{230}Th flux to ocean sediments constrained by GCM modelling, *Deep Sea Res., Part I*, *46*(11), 1861–1893, doi:10.1016/S0967-0637(99)00030-8.

Henderson, G. M., N. C. Slowey, and G. A. Haddad (1999b), Fluid flow through carbonate platforms: Constraints from ^{234}U/^{238}U and Cl^- in Bahamas pore-waters, *Earth Planet. Sci. Lett.*, *169*(1–2), 99–111, doi:10.1016/S0012-821X(99)00065-5.

Hilgen, F. J. (1991), Astronomical calibration of Gauss to Matuyama sapropels in the Mediterranean and implication for the Geomagnetic Polarity Time Scale, *Earth Planet. Sci. Lett.*, *104*(2–4), 226–244, doi:10.1016/0012-821X(91)90206-W.

Jorissen, F. J., A. Asioli, A. M. Borsetti, L. Capotondi, J. P. de Visser, F. J. Hilgen, E. J. Rohling, K. van der Borg, C. Vergnaud Grazzini, and W. J. Zachariasse (1993), Late Quaternary central Mediterranean biochronology, *Mar. Micropaleontol.*, *21*(1–3), 169–189, doi:10.1016/0377-8398(93)90014-O.

Jung, M., J. Ilmberger, A. Mangini, and K.-C. Emeis (1997), Why some Mediterranean sapropels survived burn-down (and others did not), *Mar. Geol.*, *141*(1–4), 51–60, doi:10.1016/S0025-3227(97)00031-5.

Kidd, R. B., M. B. Cita, and W. B. F. Ryan (1978), Stratigraphy of eastern Mediterranean sapropel sequences recovered during Leg 42A and their paleoenvironmental significance, *Initial Rep. Deep Sea Drill. Proj.*, *42A*, 421–443.

Klinkhammer, G. P., and M. R. Palmer (1991), Uranium in the oceans: Where it goes and why, *Geochim. Cosmochim. Acta*, *55*(7), 1799–1806, doi:10.1016/0016-7037(91)90024-Y.

Ku, T.-L. (1965), An evaluation of the ^{234}U/^{238}U method as a tool for dating pelagic sediments, *J. Geophys. Res.*, *70*(14), 3457–3474, doi:10.1029/JZ070i014p03457.

Lawrence, E. R., J. H. Chen, and G. J. Wasserburg (1987), ^{238}U-^{234}U-^{230}Th-^{232}Th systematics and the precise measurement of time over the past 500,000 years, *Earth Planet. Sci. Lett.*, *81*(2–3), 175–192, doi:10.1016/0012-821X(87)90154-3.

Li, Y.-H., and S. Gregory (1974), Diffusion of ions in sea water and in deep-sea sediments, *Geochim. Cosmochim. Acta*, *38*(5), 703–714, doi:10.1016/0016-7037(74)90145-8.

Lourens, L. J., A. Antonarakou, F. J. Hilgen, A. A. M. Van Hoof, C. Vergnaud-Grazzini, and W. J. Zachariasse (1996), Evaluation of the Plio-Pleistocene astronomical timescale, *Paleoceanography*, *11*(4), 391–413, doi:10.1029/96PA01125.

Löwemark, L., Y. Lin, H.-F. Chen, T.-N. Yang, C. Beier, F. Werner, C.-Y. Lee, S.-R. Song, and S.-J. Kao (2006), Sapropel burn-down and ichnological response to late Quaternary sapropel formation in two ~400 ky records from the eastern Mediterranean Sea, *Palaeogeogr. Palaeoclimatol. Palaeoecol.*, *239*(3–4), 406–425, doi:10.1016/j.palaeo.2006.02.013.

Mangini, A., and J. Dominik (1979), Late Quaternary sapropel on the Mediterranean Ridge: U-budget and evidence for low sedimentation rates, *Sediment. Geol.*, *23*(1–4), 113–125, doi:10.1016/0037-0738(79)90009-5.

Mangini, A., M. Jung, and S. Laukenmann (2001), What do we learn from peaks of uranium and of manganese in deep sea sediments?, *Mar. Geol.*, *177*(1–2), 63–78, doi:10.1016/S0025-3227(01)00124-4.

McManus, J., W. M. Berelson, G. P. Klinkhammer, D. E. Hammond, and C. Holm (2005), Authigenic uranium: Relationship to oxygen penetration depth and organic carbon rain, *Geochim. Cosmochim. Acta*, *69*(1), 95–108, doi:10.1016/j.gca.2004.06.023.

Mercone, D., J. Thomson, R. H. Abu-Zied, I. W. Croudace, and E. J. Rohling (2001), High-resolution geochemical and micropalaeontological profiling of the most recent eastern Mediterranean sapropel, *Mar. Geol.*, *177*(1–2), 25–44, doi:10.1016/S0025-3227(01)00122-0.

Murat, A., and H. Got (1989), Middle and late Quaternary depositional sequences and cycles in the eastern Mediterranean—Reply, *Sedimentology*, *36*(1), 156–158, doi:10.1111/j.1365-3091.1989.tb00828.x.

Nijenhuis, I. A., J. Becker, and G. J. De Lange (2001), Geochemistry of coeval marine sediments in Mediterranean ODP cores and a land section: Implications for sapropel formation models, *Palaeogeogr. Palaeoclimatol. Palaeoecol.*, *165*(1–2), 97–112, doi:10.1016/S0031-0182(00)00155-3.

Osborne, A. H., G. Marino, D. Vance, and E. J. Rohling (2010), Eastern Mediterranean surface water Nd during Eemian sapropel S5: Monitoring northerly (mid-latitude) versus southerly (sub-tropical) freshwater contributions, *Quat. Sci. Rev.*, *29*(19–20), 2473–2483, doi:10.1016/j.quascirev.2010.05.015.

Paterne, M., F. Guichard, J. Labeyrie, P. Y. Gillot, and J. C. Duplessy (1986), Tyrrhenian Sea tephrochronology of the oxygen isotope record for the past 60,000 years, *Mar. Geol.*, *72*(3–4), 259–285, doi:10.1016/0025-3227(86)90123-4.

Pates, J. M., and G. K. P. Muir (2007), U-salinity relationships in the Mediterranean: Implications for Th-234: U-238 particle flux studies, *Mar. Chem.*, *106*(3–4), 530–545, doi:10.1016/j.marchem.2007.05.006.

Pichat, S., K. W. W. Sims, R. Francois, J. F. McManus, S. B. Leger, and F. Albarede (2004), Lower export production during glacial periods in the equatorial Pacific derived from (^{231}Pa/^{230}Th)$_{xs,0}$ measurements in deep-sea sediments, *Paleoceanography*, *19*, PA4023, doi:10.1029/2003PA000994.

Reyss, J.-L., S. Schmidt, F. Legeleux, and P. Bonté (1995), Large, low background well-type detectors for measurements of environmental radioactivity, *Nucl. Instrum. Methods Phys. Res., Sect. A*, *357*(2–3), 391–397, doi:10.1016/0168-9002(95)00021-6.

Robinson, L. F., J. F. Adkins, D. P. Fernandez, D. S. Burnett, S. L. Wang, A. C. Gagnon, and N. Krakauer (2006), Primary U distribution in scleractinian corals and its implications for U series dating, *Geochem. Geophys. Geosyst.*, *7*, Q05022, doi:10.1029/2005GC001138.

Rohling, E. J. (1994), Review and new aspects concerning the formation of eastern Mediterranean sapropels, *Mar. Geol.*, *122*(1–2), 1–28, doi:10.1016/0025-3227(94)90202-X.

Rohling, E. J., E. C. Hopmans, and J. S. S. Damste (2006), Water column dynamics during the last interglacial anoxic

event in the Mediterranean (sapropel S5), *Paleoceanography*, *21*, PA2018, doi:10.1029/2005PA001237.

Severmann, S., and J. Thomson (1998), Investigation of the ingrowth of radioactive daughters of in Mediterranean sapropels as a potential dating tool, *Chem. Geol.*, *150*(3–4), 317–330, doi:10.1016/S0009-2541(98)00113-2.

Spencer, D. W., M. P. Bacon, and P. G. Brewer (1981), Models of the distribution of ^{210}Pb in a section across the north equatorial Atlantic Ocean, *J. Mar. Res.*, *39*(1), 119–138.

Stroobants, N., F. Dehairs, L. Goeyens, N. Vanderheijden, and R. van Grieken (1991), Barite formation in the Southern Ocean water column, *Mar. Chem.*, *35*, 411–421, doi:10.1016/S0304-4203(09)90033-0.

ten Haven, H. L., J. W. de Leeuw, P. A. Schenck, and G. T. Klaver (1988), Geochemistry of Mediterranean sediments. Bromine/organic carbon and uranium/organic carbon ratios as indicators for different sources of input and post-depositional oxidation, respectively, *Org. Geochem.*, *13*(1–3), 255–261, doi:10.1016/0146-6380(88)90044-7.

Thomson, J. (1982), Holocene sedimentation rates on the Hellenic outer ridge: A comparison by ^{14}C and ^{230}Th$_{excess}$ methods, *Sediment. Geol.*, *32*(1–2), 99–110, doi:10.1016/0037-0738(82)90016-1.

Thomson, J., D. Mercone, G. J. De Lange, and P. J. M. Van Santvoort (1999), Review of recent advances in the interpretation of eastern Mediterranean sapropel S1 from geochemical evidence, *Mar. Geol.*, *153*(1–4), 77–89, doi:10.1016/S0025-3227(98)00089-9.

Thunell, R. C., and D. F. Williams (1989), Glacial-Holocene salinity changes in the Mediterranean Sea: Hydrographic and depositional effects, *Nature*, *338*(6215), 493–496, doi:10.1038/338493a0.

Walter, H. J., M. M. Rutgers van der Loeff, and H. Hoeltzen (1997), Enhanced scavenging of ^{231}Pa relative to ^{230}Th in the south Atlantic south of the Polar front: Implications for the use of the ^{231}Pa/^{230}Th ratio as a paleoproductivity proxy, *Earth Planet. Sci. Lett.*, *149*(1–4), 85–100, doi:10.1016/S0012-821X(97)00068-X.

Warning, B., and H. J. Brumsack (2000), Trace metal signatures of eastern Mediterranean sapropels, *Palaeogeogr. Palaeoclimatol. Palaeoecol.*, *158*(3–4), 293–309, doi:10.1016/S0031-0182(00)00055-9.

Weldeab, S., K.-C. Emeis, C. Hemleben, G. Schmiedl, and H. Schulz (2003), Spatial productivity variations during formation of sapropels S5 and S6 in the Mediterranean Sea: Evidence from Ba contents, *Palaeogeogr. Palaeoclimatol. Palaeoecol.*, *191*(2), 169–190, doi:10.1016/S0031-0182(02)00711-3.

Yu, E. F., R. Francois, M. P. Bacon, S. Honjo, A. P. Fleer, S. J. Manganini, M. M. Rutgers van der Loeff, and V. Ittekot (2001), Trapping efficiency of bottom-tethered sediment traps estimated from the intercepted fluxes of ^{230}Th and ^{231}Pa, *Deep Sea Res., Part I*, *48*(3), 865–889, doi:10.1016/S0967-0637(00)00067-4.

Zheng, Y., R. F. Anderson, A. Van Geen, and M. Q. Fleisher (2002), Preservation of particulate non-lithogenic uranium in marine sediments, *Geochim. Cosmochim. Acta*, *66*(17), 3085–3092, doi:10.1016/S0016-7037(01)00632-9.